Solvent Effects on NMR Isotropic Shielding Constants. A Comparison between Explicit Polarizable Discrete and Continuum Approaches

Kestutis Aidas, Andreas Møgelhøj, Hanna Kjær, Christian B. Nielsen,† and Kurt V. Mikkelsen

Department of Chemistry, H. C. Ørsted Institute, University of Copenhagen, Universitetsparken 5, DK-2100 Copenhagen Ø, Denmark

Kenneth Ruud

Center for Theoretical and Computational Chemistry (CTCC), Department of Chemistry, University of Tromsø, N-9037 Tromsø, Norway

Ove Christiansen

The Lundbeck Foundation Center for Theoretical Chemistry, Department of Chemistry, University of Aarhus, Langelandsgade 140, DK-8000 Aarhus C, Denmark

Jacob Kongsted*

Department of Theoretical Chemistry, Chemical Center, University of Lund, P.O. Box 124, S-221 00 Lund, Sweden

Received: December 18, 2006; In Final Form: March 14, 2007

The gas-to-aqueous solution shifts of the ^{17}O and ^{13}C NMR isotropic shielding constants for the carbonyl chromophore in formaldehyde and acetone are investigated. For the condensed-phase problem, we use the hybrid density functional theory/molecular mechanics approach in combination with a statistical averaging over an appropriate number of solute−solvent configurations extracted from classical molecular dynamics simulations. The PBE0 exchange-correlation functional and the 6-311++G(2d,2p) basis set are used for the calculation of the shielding constants. London atomic orbitals are employed to ensure gauge-origin independent results. The effects of the bulk solvent molecules are found to be crucial in order to calculate accurate solvation shifts of the shielding constants. Very good agreement between the computed and experimental solvation shifts is obtained for the shielding constants of acetone when a polarizable water potential is used. Supermolecular results based on geometry-optimized molecular structures are presented. We also compare the results obtained with the polarizable continuum model to the results obtained using explicit MM molecules to model the bulk solvent effect.

I. Introduction

Although modern electronic structure methods can describe small- to medium-sized molecules in the gas phase with a high degree of accuracy, the modeling of molecules in the condensed phase still is a great challenge to ab initio theory. The construction and benchmarking of solvent models is therefore an important research area by its own merits, in addition to being important for establishing reliable protocols for calculating molecular properties in solutions. Solvent models may be classified into three main branches: (i) discrete cluster models (the supermolecular approach[1−3] and combined quantum mechanics/molecular mechanics (QM/MM) methods[4−7]), (ii) continuum models,[8,9] and (iii) molecular dynamics (MD) simulations comprising classical MD,[10] Monte Carlo[10] (MC), and Car-Parrinello MD[11] (CPMD) simulations. All of these models are very different in the way they are formulated and have their own advantages and disadvantages.

Among the different solvent methods available, we find the QM/MM model particularly attractive. In the QM/MM scheme, the molecular system is divided into at least two parts. A part of the system, for example, the solute molecule, is described by a quantum mechanical (QM) method while the other part, for example, the solvent molecules, is described by a simple molecular mechanics (MM) model. Because MM methods are computationally cheap, a large number of solvent molecules may be included in the system, allowing the discrete nature of the liquid to be preserved in the calculation. The QM/MM calculations may be used in combination with MD or MC simulations. In these cases, the QM/MM scheme is applied for a number of solute−solvent configurations extracted from the MD or MC simulation. The relevant molecular property is then obtained by statistical averaging over the configurations. This approach also takes into account the dynamical character of the liquid.

Recently, a QM/MM scheme was implemented in the electronic structure program Dalton,[12] where the QM part of the system was treated at the coupled-cluster level of theory (the CC/MM model[13]) and successfully applied to a variety of

* To whom all correspondence should be addressed. E-mail: Jacob.Kongsted@teokem.lu.se.

† Present address: Laboratory of Macromolecular and Organic Chemistry, Eindhoven University of Technology, P.O. Box 513, 5600 MB, Eindhoven, The Netherlands.

10.1021/jp068693e CCC: $37.00
Published on Web 05/03/2007

electric molecular properties.[14−19] The code has recently been extended to a combined density functional theory[20]/molecular mechanics (DFT/MM) method, allowing larger molecular systems to be investigated.[21] For both the CC/MM and DFT/MM methods, the effect of explicit solvent polarization is accounted for in the optimization of the wave function (or Kohn−Sham orbitals and therefore the electron density in the case of DFT/MM). In this paper, we apply the DFT/MM method within a gauge-origin independent scheme to calculate the gas-to-aqueous solution shifts of the ^{17}O and ^{13}C nuclear magnetic resonance (NMR) chemical shifts of the carbonyl chromophore in formaldehyde and acetone. This is motivated by the importance of NMR spectroscopy in investigations of molecular structure and dynamics as well as its widespread use in the fields of chemistry and biology.[22−24] The theoretical determination of NMR parameters is therefore important because it often serves as a valuable support in the interpretation of experimental NMR spectra.

The applicability and necessity of the high-end theoretical methods such as CC for quantitative accuracy of predicted NMR shieldings is well-known from theoretical benchmark calculations and comparisons to experiment.[25−27] In this study, we use DFT because DFT/MM is now available for the calculation of shielding constants.[28] Though DFT cannot match the quantitative predictive power of high-level CC methods, we argue and demonstrate that the solvation shifts may be predicted fairly well by this approach. The DFT/MM method used for the calculation of nuclear shielding constants is formulated in the basis of gauge-including atomic orbitals (GIAO),[29−32] also denoted London atomic orbitals, to ensure origin-independent results. The shielding constants in the liquid phase are obtained by applying the (GIAO)-DFT/MM method for a number of molecular snapshots taken from a MD simulation.

Formaldehyde and acetone are the smallest molecules having the chemically important carbonyl group and are therefore convenient test molecules for a solvation model. In the case of formaldehyde in water, a comparison with experimental data is hardly possible because formaldehyde is very reactive and forms adducts with the solvent. However, some theoretical calculations have been published for this system (see ref 33 and references therein), which can be used for comparative purposes. In contrast, acetone is stable in water, and reliable experimental data exist. The experimental gas-to-aqueous solution shifts of the ^{17}O and ^{13}C NMR chemical shifts of the carbonyl chromophore in acetone are 75.5 and −18.9 ppm,[34,35] respectively. With respect to molecular magnetic properties, acetone in aqueous solution has been studied theoretically at the DFT level where the solvent effects were described by MD or CPMD combined with a dielectric continuum,[34,36,37] or using QM/MM and dielectric continuum[38] models. Reference 38 also contains a MP2 study of the corresponding shifts. However, the study in ref 38 used a nonpolarizable force field only.

The magnetic shielding constants of a molecule in the gas phase are usually different from those in solution. The solvent effect on the magnetic shielding constants is often phenomenologically partitioned as[39]

$$\Delta\sigma_{solv} = \sigma_{sol} - \sigma_{vac} = \Delta\sigma_{bulk} + \Delta\sigma_{an} + \Delta\sigma_{polar} + \Delta\sigma_{vdw} \qquad (1)$$

The first term, $\Delta\sigma_{bulk}$, comes from the macroscopic magnetic susceptibility of the solvent. It has a constant value for samples of cylindrical shape (the usual shape of the tube in NMR experiments), and the experimental spectra are usually corrected for this term.[34] The second contribution, $\Delta\sigma_{an}$, arises from the anisotropy of the magnetic susceptibility of the solvent molecules close to the solute. In electronic structure calculations, this term can be accounted for by including a number of explicit solvent molecules in the system. The third contribution, $\Delta\sigma_{polar}$, is due to the electrostatic solute−solvent interactions. This is a long-range effect, and a large number of solvent molecules should be considered in order to take it into account properly. The change in the shielding constants due to geometrical distortions of the solute can also be incorporated into this term and potentially also the effect of formation of hydrogen bonds. Finally, $\Delta\sigma_{vdw}$ refers to the change due to the van der Waals, that is, dispersion and short-range repulsion, interactions. In this study, the $\Delta\sigma_{polar}$ term is expected to be predominant because we are dealing with water, which is a highly polar solvent where strong hydrogen bonds are formed. However, for accurate predictions of the solvation shift of magnetic shielding constants, the $\Delta\sigma_{vdw}$ contribution may also be important.

The paper is organized in the following way. In the next section, we briefly outline the methods used. In Section III, the results and a discussion of the choice of exchange-correlation functional and basis set, the details of the MD simulation, and the actual DFT/MM calculations are presented. Finally, the main findings are summarized in the last section.

II. Method

For the calculation of the nuclear magnetic shielding tensors both in vacuum and in solution, we apply linear response DFT.[40,41] GIAOs are used to ensure gauge-origin independence of the results. For a description of the theoretical and implementational aspects of the (GIAO)-DFT/MM method, we refer to our previous works.[21,28] Classical MD simulations were performed in order to generate a number of statistically uncorrelated molecular solute−solvent configurations. The potential used in the MD simulation accounts explicitly for the electric polarization, that is, partial atomic point charges and an electric polarizability tensor are assigned to each molecule in the MD simulation. We have also conducted the MD simulation using a potential that treats the electric polarization implicitly. In this case, classical molecules adopt partial atomic point charges of increased magnitudes as compared to the polarizable potential. The explicit introduction of many-body effects leads, however, to an enhanced cooperativity of the solvent molecules around the solute. A spherical cutoff radius is then adopted for each molecular configuration dumped in the MD simulation. Subsequently, the molecular configurations obtained are used in the DFT/MM calculations of the magnetic shielding tensors. Here we apply (GIAO)-DFT for the solute molecule (or potentially the solute plus a few solvent molecules), whereas the rest of the solvent molecules are described classically. In the DFT/MM calculations, we use the same potential (force field) as in the MD simulation. The explicit treatment of the solvent polarization in the QM/MM scheme has previously been shown to be very important for the accurate calculation of a number of molecular electric properties in the condensed phase.[14−17] In this work, we test the performance of the polarizable and nonpolarizable force fields in the prediction of NMR shielding constants of molecules in solution. The isotropic shielding constant in aqueous solution is obtained by a statistical averaging over all configurations. Finally, the gas-to-aqueous solution shift of the isotropic shielding constant is determined as the difference in the shielding constants between aqueous solution and vacuum. In all calculations of the magnetic shielding tensor, rovibrational effects are not taken into account, assuming that this effect cancels in the calculation of the gas-to-liquid shifts. In addition, relativistic effects have also been neglected.

TABLE 1: Structural Data and Labeling for Formaldehyde and Acetone[a]

	exp[b]	vacuum	2w/DC	MD sim
		H_2CO		
labeling		for-vac	for+2w/DC	for-sim[c]
r(OC)	1.203 ± 0.003	1.200	1.212	1.211
r(CH)	1.099 ± 0.009	1.105	1.101	1.101
∠(HCH)	116.5 ± 1.2	116.3	117.4	116.2
		$(CH_3)_2CO$		
labeling		act-vac	act+2w/DC	act-sim
r(OC1)	1.210 ± 0.003	1.210	1.225	1.218
r(C1C2)	1.507 ± 0.002	1.514	1.501	1.508
r(C2H1)	1.076 ± 0.006	1.087	1.087	1.087
r(C2H2)	1.076 ± 0.006	1.092		1.092
∠(C1C2C1)	116.7 ± 0.3	116.6	117.3	116.7
∠(C1C2H1)	111.7 ± 1.5	110.1	111.2	110.7
∠(C1C2H2)	111.7 ± 1.5	110.2		109.8
∠(OC1C2H1)	0.0[d]	0.0	8.2	0.0
∠(OC1C2H2)		121.2		121.5

[a] Bond lengths in Å, angles in deg. PCM is used for the DC model. The geometrical parameters of water molecules in the 2w/DC structures are not reported. [b] Experimental gas-phase geometries of formaldehyde and acetone are taken from refs 71 and 72, respectively. [c] From ref 62. [d] In contrast to ref 72, the C_{2v} symmetry of acetone in gas phase is assumed.

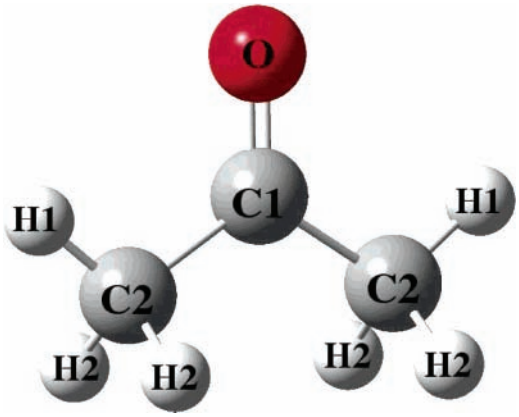

Figure 1. Definition of the atomic labels used for the acetone molecule.

The MD simulations were performed using the MOLSIM program.[42] The DFT/MM calculations have been performed using the Dalton quantum chemistry program package.[12] The MidasCpp program[43] was used to generate inputs to Dalton as well as to perform the statistical analysis. The Gaussian 03 suite of programs[44] was used for all geometry optimizations.

III. Results and Discussion

A. Method Analysis. For accurate calculations of isotropic shielding constants, an appropriate DFT functional should be chosen as well as a suitable basis set. To investigate how the isotropic shielding constants and the corresponding solvation shifts vary with the DFT functional and basis set, we have first optimized the vacuum and liquid-phase geometries of formaldehyde and acetone. The vacuum geometries of both molecules were optimized at the B3LYP[45]/aug-cc-pVTZ[46] level of theory and are tabulated in Table 1. In this table, we also introduce the notation used for labeling the different structures of formaldehyde and acetone used in this work. The atom labeling for acetone is presented in Figure 1. Both compounds have C_{2v} symmetry in vacuum, and the calculated structures compare fairly well with the experimental geometries. In addition, the computed gas-phase electric dipole moments of 2.390 and 3.080 D for formaldehyde and acetone, respectively, are in reasonable agreement with the experimental values of 2.339 ± 0.013 D[47] and 2.88 D.[48] The liquid-phase geometries were obtained by optimizing a cluster consisting of formaldehyde/acetone and two water molecules hydrogen bonded to the oxygen atom of the carbonyl group at the B3LYP/aug-cc-pVTZ level together with the polarizable continuum model[49] (PCM). The aggregate of formaldehyde and two water molecules retains the C_{2v} symmetry. However, the geometry optimization of acetone and two water molecules leads to a twisting of the methyl groups in acetone, thereby reducing the symmetry of the aggregate (and acetone itself) to C_2 symmetry. In the latter structure, the hydrogen atoms in the same methyl group are no longer equivalent because of the reduced symmetry, and Table 1 only contains the data for the hydrogen having the smallest dihedral angle with respect to the C2−C1−O frame of the acetone molecule. The considerable elongation of the CO bond length of formaldehyde and acetone is the most important consequence of the aggregation.

Several DFT exchange-correlation functionals including B3LYP,[45] PBE0,[50] OLYP,[51] KT2,[52,53] and KT3[54] have been tested by calculating the ^{17}O and ^{13}C isotropic shielding constants of formaldehyde for its vacuum and for+2w/DC geometries given in Table 1. The computed numbers are collected in Table 2. For the for+2w/DC system, the water molecules were considered either classically by applying the DFT/MM method or at the same DFT level as the isolated formaldehyde molecule. For the DFT/MM scheme, we use the SPCpol potential for the water molecules (vide infra, see Table 7). The basis set used was aug-cc-pCVTZ.[55] We denote the ^{17}O and ^{13}C isotropic shielding constants of the carbonyl chromophore in formaldehyde and acetone by σ^O and σ^C, respectively. Similarly, the solvation shifts are denoted δ^O and δ^C. The solvation shifts of the isotropic shielding constants are defined as $\delta^X(\text{DFT/MM}) = \sigma^X_{\text{for+2w/DC}}(\text{DFT/MM}) - \sigma^X_{\text{for−vac}}(\text{DFT})$ and $\delta^X(\text{DFT}) = \sigma^X_{\text{for+2w/DC}}(\text{DFT}) - \sigma^X_{\text{for−vac}}(\text{DFT})$, for $X = O, C$. The results are collected in Table 3. The term δ^X(DFT/MM) only accounts for the $\Delta\sigma_{\text{polar}}$ contribution in the decomposition of the solvent effects on shielding constants as given in eq 1, whereas δ^X(DFT) also includes, to some extent, the effect of $\Delta\sigma_{\text{vdw}}$ and $\Delta\sigma_{\text{an}}$. As seen from Table 3, the pure electrostatic intermolecular interactions are responsible for the major part of the solvent shift in the isotropic shielding constants. The nonclassical interactions have a rather small effect on δ^O with a tendency to increase it, and these effects are even

TABLE 2: Isotropic Shielding Constants σ^O and σ^C of Formaldehyde (in ppm) Calculated Using Various DFT Functionals and MP2 Method in Combination with the aug-cc-pCVTZ Basis Set[a]

structure	method	B3LYP	PBE0	OLYP	KT2	KT3	MP2
			σ^O				
for-vac	QM	−436.5	−437.3	−401.0	−368.3	−358.9	−314.2
for+2w/DC	QM/MM	−381.8	−381.9	−353.3	−323.4	−314.9	
for+2w/DC	QM	−376.7	−374.9	−351.5	−317.1	−312.1	−279.5
			σ^C				
for-vac	QM	−20.7	−17.9	−14.1	−2.5	−1.4	9.4
for+2w/DC	QM/MM	−31.2	−28.3	−23.6	−11.9	−10.5	
for+2w/DC	QM	−31.0	−28.3	−22.8	−11.9	−10.1	0.1

[a] In the for+2w/DC structure, the water molecules were treated either classically (QM/MM) or quantum mechanically (QM).

TABLE 3: Solvation Shifts of the Isotropic Shielding Constants δ^O and δ^C in Formaldehyde (in ppm) Computed Using the Data in Table 2

	B3LYP	PBE0	OLYP	KT2	KT3	MP2
			δ^O			
QM/MM	54.7	55.4	47.7	44.9	44.0	
QM	59.8	62.4	49.5	51.2	46.8	34.7
			δ^C			
QM/MM	−10.5	−10.4	−9.5	−9.4	−9.1	
QM	−10.3	−10.4	−8.7	−9.4	−8.7	−9.3

smaller for δ^C. We therefore conclude that the DFT/MM scheme with solvent molecules treated classically should be capable of accurately predicting the solvation shifts of the shieldings in formaldehyde and acetone.

We note that relatively similar solvation shifts are obtained with the different functionals, even though the absolute results are very different. This is important in the present context because we cannot claim that the DFT results give high quantitative accuracy for the absolute values of the isotropic shielding constants. In fact, the opposite has been demonstrated by Auer et al.,[25] for example, for the B3LYP functional, in careful benchmark calculations against highly accurate CC results for the ^{13}C shielding constants in vacuum. Also, to the best of our knowledge there are no systematic investigations on the comparison between DFT and, for instance, CC solvation shifts for NMR shielding constants reported in the literature. In Tables 2 and 3 we have inserted the MP2[56] results for, respectively, absolute shielding constants, $\sigma^O$and σ^C, and solvation shifts, $\delta^O$and δ^C, of formaldehyde. Here we have performed only the full (GIAO)-MP2 calculations on the for-vac and the for-2w/DC geometries using the Gaussian 03 program. As seen from Table 3, the MP2 solvation shift δ^O is somewhat smaller than the DFT shift, whereas the δ^C shifts are very close. The discrepancy between MP2 and DFT δ^O shifts probably arises mainly due to the van der Waals interactions, which are known to be treated rather poorly by the DFT methods employed in this work.[57] It might be, however, that the MP2 method overestimates this contribution leading to the underestimated shifts. This makes the comparison between MP2 and DFT results somewhat complicated. Therefore, accurate CC calculations would be of great help in assessing the van der Waals contribution to the solvation shifts of NMR shielding constants, which will be the subject of our forthcoming work. However, the fact that the solvation shift is fairly constant for the different functionals lends some support to using DFT as an approach to calculate the solvation shift of the shielding constants. Furthermore, we keep in mind the well-known cost efficiency of DFT in relation to calculations of structures, energies, and molecular properties. The PBE0 functional was chosen for the subsequent calculations in this study because this functional has been used successfully for calculating shielding constants for a number of molecules in the gas phase,[58] and in refs 34 and 36−38 this functional was also applied for the calculation of the gas-to-aqueous solution shift of σ^O and σ^C of the carbonyl chromophore in acetone, with satisfactory results.

In Table 4, we present the PBE0 σ^O and σ^C values of formaldehyde for different basis sets. For each entry in Table 4, the number of contracted basis functions is given. We have investigated two correlation-consistent basis set families aug-cc-pVXZ[46] and aug-cc-pCVXZ[55] with X = D,T,Q, denoted here as axz and acxz, respectively. The Pople-type basis set 6-311++G(2d,2p)[59] was also tested. We designate the latter basis set as *P*1. Three structures have been employed in the basis-set analysis: (1) the vacuum structure of formaldehyde (for-vac), (2) the for+2w/DC geometry of formaldehyde with two water molecules, and (3) the for+2w/DC structure of only formaldehyde, that is, with both water molecules removed, and therefore designated for* in Table 4. For the for+2w/DC aggregate, the DFT/MM model was applied with the SPCpol parameters for the water molecules. A systematic decrease in the value of the isotropic shielding constants is observed in the sequences (a(c)xz) and (axz,acxz), x = d,t,q, that is, with increasing basis set size and flexibility. However, even the actz or aqz results for σ^O and σ^C cannot be considered to be converged with respect to the corresponding acqz numbers. Actually, even the cc-pV6Z basis at the DFT level does not guarantee converged values for the σ^O and σ^C of formaldehyde.[33] However, a different picture emerges if we consider the solvation shifts of the shielding constants (Table 5). For the data in Table 4, the shifts $\delta^X_{geom} = \sigma^X_{for^*} - \sigma^X_{for-vac}$, $\delta^X_{solv} = \sigma^X_{for+2w/DC} - \sigma^X_{for^*}$, and $\delta^X_{total} = \sigma^X_{for+2w/DC} - \sigma^X_{for-vac}$, ($X$ = O, C) for the isotropic shielding constants can be defined. δ^X_{geom} shows how the shielding constant is changed due to the distortions in the geometry of formaldehyde caused by its aggregation with two water molecules. δ^X_{solv} corresponds to the shift due to the solvation of formaldehyde by two classical water molecules, and finally δ^X_{total} accounts for the total shift due to both the geometrical distortions and the solvation. The numbers in Table 5 show a smooth convergence of the shifts in the shielding constants. The change in the total shift is less than 1 ppm when moving from the actz to the corresponding acqz numbers. This indicates that the errors in the calculation of the shielding constants cancel in the calculation of the shifts. In agreement with the findings of ref 34, the PBE0/6-311++G-(2d,2p) shifts are very close to the values obtained using the extensive actz and acqz basis sets. The 6-311++G(2d,2p) basis set is rather small, and the computational time using this basis set versus, for instance, the actz basis set is reduced by a factor of ∼12. Therefore, in the following we will use the PBE0 functional combined with the 6-311++G(2d,2p) basis set in all calculations of the shifts of the isotropic shielding constants for formaldehyde and acetone.

TABLE 4: PBE0 Basis Set Dependence of the Isotropic Shielding Constants σ^O and σ^C of Formaldehyde (in ppm)[a]

structure	adz	atz	aqz	acdz	actz	acqz	*P*1
no. of basis funcs.	64	138	252	72	164	310	74
			σ^O				
for-vac	−387.4	−424.3	−440.3	−405.1	−437.3	−446.9	−432.3
for*	−408.7	−446.6	−463.1	−426.9	−460.0	−469.9	−454.9
for+2w/DC	−334.5	−369.9	−384.6	−351.2	−381.9	−390.8	−376.1
			σ^C				
for-vac	1.6	−11.7	−18.1	−6.1	−17.9	−21.0	−12.8
for*	−2.2	−15.8	−22.3	−10.0	−22.1	−25.3	−16.9
for+2w/DC	−7.6	−21.9	−28.5	−15.7	−28.3	−31.6	−23.1

[a] The structure denoted for* corresponds to the structure of formaldehyde as in the for+2w/DC system, but with the water molecules removed. The DFT/MM model was applied for the for+2w/DC system including both water molecules in the MM part.

TABLE 5: Geometrical (δ_{geom}), Pure Solvation (δ_{solv}) and Total Solvation (δ_{total}) Shifts in Isotropic Shielding Constants for Different Basis Sets (in ppm)[a]

	adz	atz	aqz	acdz	actz	acqz	*P*1
			δ^O				
δ_{geom}	−21.3	−22.3	−22.8	−21.8	−22.7	−23.0	−22.6
δ_{solv}	74.2	76.7	78.5	75.7	78.1	79.1	78.8
δ_{total}	52.9	54.4	55.7	53.9	55.4	56.1	56.2
			δ^C				
δ_{geom}	−3.8	−4.1	−4.2	−3.9	−4.2	−4.3	−4.1
δ_{solv}	−5.4	−6.1	−6.2	−5.7	−6.2	−6.3	−6.2
δ_{total}	−9.2	−10.2	−10.4	−9.6	−10.4	−10.6	−10.3

[a] The table was compiled using the data in Table 4. See the text for comments and definitions of δ_{geom}, δ_{solv}, and δ_{total}.

TABLE 6: PBE0/6-311++G(2d,2p) Isotropic Shielding Constants, σ^O and σ^C, and the Solvation Shifts in σ^O and σ^C, δ^O and δ^C, (in ppm) Calculated for Different Structures of Acetone[a]

structure	method	σ^O	δ^O	σ^C	δ^C
act-vac	DFT	−339.2		−21.5	
act*	DFT	−355.7	−16.5	−26.2	−4.7
act+2w/DC	DFT/MM	−282.7	56.5	−33.5	−12.0
act+2w/DC	DFT	−276.2	63.0	−35.3	−13.8
act+2w/DC	DFT/PCM-UA0	−245.5	93.7	−39.7	−18.2
act+2w/DC	DFT/PCM-UFF	−233.0	106.2	−41.0	−19.5
act-sim	DFT/PCM-UA0	−285.6	53.6	−33.2	−11.7
exp			75.5		−18.9

[a] See the text for comments.

B. Supermolecular Results. The supermolecular approach is a widely used method to study different molecular properties in condensed phases. This method involves the geometry optimization of the solute together with one or more solvent molecules. In addition, the dielectric continuum model may be applied to include the long-range electrostatic bulk effects. This procedure leads to energy-minimized structures of the aggregate. The dynamical character of the liquid, or more precisely, the molecular statistical ensemble, is therefore neglected in this approach. The energy-minimized structures can, however, certainly not be realized in the true liquid. Such an approach would therefore most likely result in an overestimation of the solvent effects. However, in the supermolecular approach, only a small number of solvent molecules is usually included in the geometry optimization, thereby neglecting the effects of long-range intermolecular interactions. The dielectric continuum model is not always capable of accounting for this contribution because it neglects the discrete nature of the liquids. The magnitude and sign of these two distinct errors determine the success of the approach. In view of these considerations, the results of the supermolecular approach should be treated with some care.

The PBE0/6-311++G(2d,2p) results obtained for the solvation shifts of σ^O and σ^C for the energy-minimized structures of acetone are presented in Table 6, where the shifts δ^O and δ^C are calculated with respect to the values σ^O and σ^C for the vacuum geometry of acetone. As in the case of formaldehyde, we observe a rather strong effect of the geometry distortions on σ^O and a somewhat smaller effect on σ^C amounting to −16.5 and −4.7 ppm, respectively. Within the DFT/MM scheme, the major part of the solvation shift comes from the electrostatic interactions of acetone with the classical water molecules, the total shifts for δ^O and δ^C being 56.5 and −12.0 ppm, respectively, which is a significant underestimate with respect to the experimental values. The quantum-mechanical effects on the shifts estimated by considering the act+2w/DC structure at the DFT level are rather small (7.5 ppm for δ^O and −1.8 ppm for δ^C), which means that the rest of the shift should be reproduced by taking more solvent molecules into consideration.

Using the Gaussian 03 program, we have also included the polarizable continuum model in the calculation of the shielding constants on the act+2w/DC structure (using default settings). In this case, the δ^O is overestimated by 18.2 ppm as compared to experimental data, whereas δ^C is reproduced rather accurately. In the default PCM framework, as implemented in the Gaussian 03 program, the interlocking spheres are constructed on each heavy atom in the molecular system according to the united atom model (UA0). Hydrogen atoms are confined within the sphere of the atom to which they are bonded. However, for the small hydrogen-bonded molecular complexes considered here, it would be natural to build spheres around hydrogens involved in hydrogen-bonding explicitly. Such a procedure would, to some extent, account for the directionality of the hydrogen bonds. Therefore, we repeated this calculation using the universal force field (UFF) scheme for the construction of the cavities in the PCM, as implemented in the Gaussian 03 program. As indicated in Table 6, δ^O is even further away from the experimental value by an additional 12.5 ppm compared to the corresponding number obtained with the PCM-UA0 model. Similarly, the PCM-UFF δ^C is slightly larger compared to the PCM-UA0 result but still in good agreement with experimental data.

As discussed in refs 34, 60, and 61, larger cavity radii may be employed in the PCM model in order to improve the results for shielding constants. Comparing the solvation shifts δ^O and δ^C for acetone calculated with and without PCM, we see that it might, in principle, be possible to adjust the shape of the cavity in order to reproduce the experimental value of δ^O. However, the enlargement of the cavity on carbon would probably lead to the degradation of the results for δ^C. A proper calibration of the PCM cavities for the calculation of NMR shielding constants is therefore an important point to consider. However, the adjustment of cavities suitable for small hydrogen-bonded

TABLE 7: Force Field Parameters for Formaldehyde, Acetone and Water Used in the MD Simulation

molecule	model	atom	charge (au)	polarizability[a] (Å^3)	σ (Å)	ϵ (kcal/mol)
H_2CO	SPC	O	−0.5760		2.850	0.8368
		C	0.3310		3.296	0.5021
		H	0.1230		2.744	0.0420
$(CH_3)_2CO$	SPCpol	O	−0.5559	0.000 0.000 0.000	2.960	0.2100
		C1	0.6985	5.083 6.905 7.015	3.750	0.1050
		C2	−0.3392	0.000 0.000 0.000	3.910	0.1600
		H1	0.0987	0.000 0.000 0.000	0.000	0.0000
		H2	0.0846	0.000 0.000 0.000	0.000	0.0000
$(CH_3)_2CO$	SPC	O	−0.65188		2.960	0.2100
		C1	0.75236		3.750	0.1050
		C2	−0.36304		3.910	0.1600
		H1	0.09970		0.000	0.0000
		H2	0.10655		0.000	0.0000
H_2O	SPCpol	O	−0.6690	1.440 1.440 1.440	3.166	0.1555
		H	0.3345	0.000 0.000 0.000	0.000	0.0000
H_2O	TIP3P	O	−0.8340		3.1507	0.1521
		H	0.4170		0.000	0.0000

[a] The diagonal components of the polarizability tensor in the order of (α_{xx}, α_{yy}, α_{zz}).

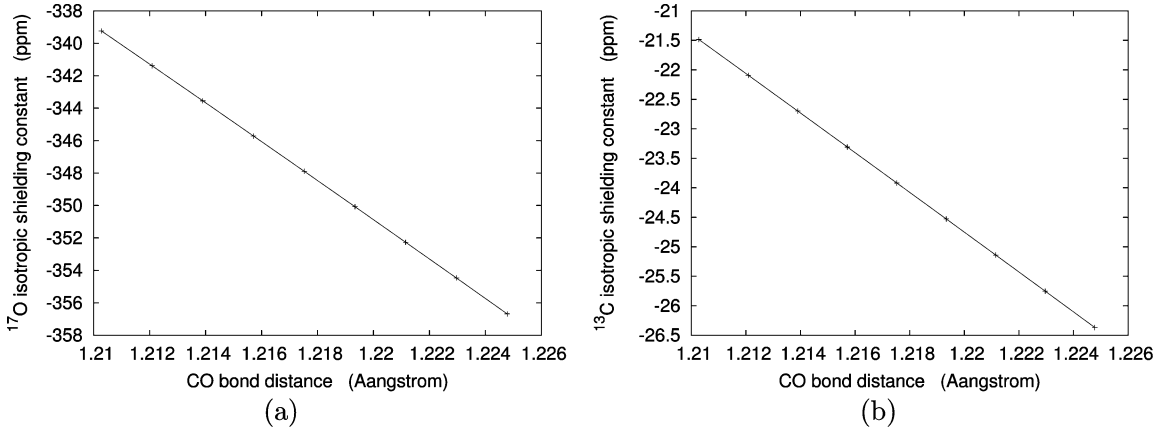

Figure 2. σ^O (a) and σ^C (b) of the carbonyl chromophore in acetone as a function of the CO bond length. Results refer to PBE0/6-311++G(2d,2p).

aggregates might be difficult. Our results clearly illustrate the limitations of the supermolecular approach. The main conclusion to be drawn at this point is that two water molecules treated either classically or quantum mechanically are obviously not enough to describe solvent effects on δ^O and δ^C, and molecular systems including a larger number of solvent molecules have to be considered.

Returning to Table 5, we recognize two effects changing the isotropic shielding constant within the DFT/MM scheme—the geometrical distortions of the solute and the electrostatic interactions with the water molecules. As seen from Table 5, these two effects are additive. We recall that the main change in the geometry of formaldehyde and acetone due to solvation is an elongation of the CO bond length. In Figure 2, the dependence of the σ^O and σ^C of the carbonyl chromophore in acetone on the CO bond length is presented. The CO bond length of acetone was varied between its value in vacuum and act+2w/DC structure reported in Table 1. A linear dependence of the shielding constants on the CO bond length is observed, and the elongation of the CO bond length by 0.01 Å results in a reduction of σ^O and σ^C by approximately 12 and 3.4 ppm, respectively. For formaldehyde, analogous linear dependencies were found with an even stronger reduction of about 15 ppm in σ^O upon elongation of the CO bond length by 0.01 Å. It is therefore mandatory to have accurate liquid-phase geometries for formaldehyde and acetone in order to obtain accurate values for the gas-to-aqueous solution shifts of the shielding constants.

Because the energy-minimized solute−solvent structures lead to an overestimation of the solvent effects, we believe that the CO bond length in the optimized 2w/DC geometries of formaldehyde and acetone is overestimated compared to the true solvent structure. In the subsequent MD simulations and DFT/MM calculations on large molecular samples, we therefore use the acetone geometry found when optimizing a single acetone in the presence of the PCM at the B3LYP/aug-cc-pVTZ level of theory. The geometrical parameters of this new liquid-phase geometry of acetone are presented in the last column of Table 1. We see that the CO bond length is in between those found in vacuum and for the act+2w/DC structure of acetone. Furthermore, in this way we also avoid the undesired C_2 symmetry found in the act+2w/DC structure of acetone. We have performed calculations using the liquid-phase geometry (and potential) of formaldehyde as derived in ref 62.

Finally, we want to complete our survey of the supermolecular results by calculating the solvation shifts δ^O and δ^C for the act-sim geometry of acetone. In this calculation, we use PCM for the effects of bulk water, thereby neglecting the explicit hydrogen bonding. As expected, this approach leads to a considerable underestimation of the corresponding solvation shifts (Table 6). These results are in line with the well-known limitation of DC models to capture effects due to hydrogen bonding.

C. MD Simulation. In the previous section, we noted the need to consider a large number of solvent molecules around the solute in order to properly describe solvent effects. In this study, we perform classical MD simulations to generate an appropriate number of solute−solvent configurations. For each selected configuration, a DFT/MM calculation is performed, and

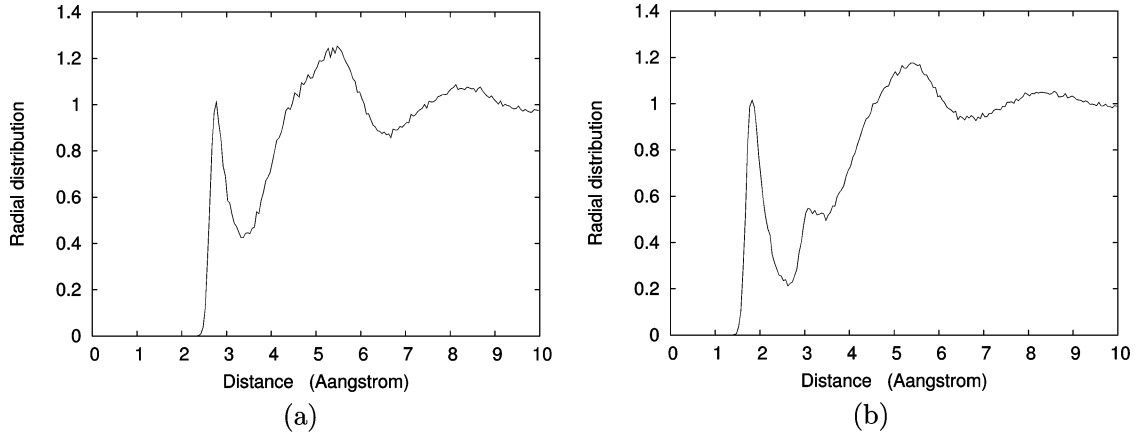

Figure 3. $O((CH_3)_2CO)-O(H_2O)$ (a) and $O((CH_3)_2CO)-H(H_2O)$ (b) radial distribution functions derived from the SPCpol MD simulation of acetone in water.

the final results are obtained by statistical averaging over all configurations. In this way, the dynamical character of the liquid is preserved.

The force field parameters for formaldehyde, acetone, and water are collected in Table 7. The geometries of formaldehyde and acetone are tabulated in Table 1 under the heading "MD sim". As mentioned above, the geometry of acetone was obtained by geometry optimization at the B3LYP/aug-cc-pVTZ level in the presence of the PCM. For the geometry and force field parameters of formaldehyde we refer to ref 62, where the electronic transition energy of formaldehyde in aqueous solution was considered within the combined CC/MM method. The geometrical parameters for water, $R(\mathrm{OH}) = 0.9572$ Å, $\angle(\mathrm{HOH}) = 104.49°$, are taken from ref 63.

In this work, we use both an explicit and an implicit treatment of the molecular polarization. In the case of the polarizable potential, we assign atomic point charges as well as dipole polarizabilities to each molecule in the MD simulation. The corresponding molecular potential is therefore denoted by the abbreviation SPCpol (simple point charge plus polarization). The SPCpol atomic point charges for acetone are derived from the CHelpG procedure[64] as implemented in the Gaussian 03 program at the B3LYP/aug-cc-pVTZ level of theory using the act-sim geometry of acetone in vacuum. In the latter calculation, we also constrain the electric dipole moment to its QM value. The polarizability tensor of acetone was obtained at the same level of theory. The dipole polarizability tensor is placed at the carbon site of the carbonyl group in acetone. The CHelpG procedure at the B3LYP/aug-cc-pVTZ level of theory together with the constraints on the electric dipole moment was also applied to derive the point charges for the nonpolarizable potential. In this case, the CHelpG point charges were obtained in the presence of the PCM and thereby they have enhanced values as compared to the vacuum charges. The nonpolarizable molecular potential is designated by the abbreviation SPC. The values of the point charges and the components of the isotropic polarizability in the SPCpol potential for water are due to Ahlström et al.[65] We place the polarizability at the oxygen site. For the nonpolarizable potential of water, we use the TIP3P potential,[66] which is of SPC type. In addition to the Coulomb potential, the SPCpol and SPC potentials also include van der Waals dispersion and repulsion parameters, σ and ϵ. Here we use a 6−12-type Lennard−Jones (LJ) potential together with Lorentz−Berthelot mixing rules.[10] The LJ parameters for acetone and water reported in the last two columns of Table 7 are the OPLS parameters from ref 67.

Both the SPCpol and SPC MD simulations were performed in a cubic box containing 1 rigid formaldehyde/acetone molecule and 511 rigid water molecules at 298.15 K. We use a time step of 2 fs in the simulation and periodic boundary conditions. The initial equilibration was carried out for 600 ps followed by a production run of 1.2 ns. The solute−solvent configurations were dumped every 1 ps. In this way, we obtain 1200 molecular configurations to be used in the combined DFT/MM calculations. Furthermore, a spherical cutoff radius of 12 Å was applied for each molecular configuration extracted from the MD simulation. As will be demonstrated later, this cutoff distance gives sufficiently converged shielding constants with respect to the number of solvent molecules included into the molecular configuration. The MOLSIM program[42] was used for the MD simulations.

As an example, we have plotted the radial distribution functions (RDFs) for the carbonyl oxygen of acetone and the water oxygen (a) and the water hydrogen (b) derived from the SPCpol MD simulation in Figure 3. A hydrogen bond peak is seen to start around 1.43 Å in the O−H RDF and around 2.38 Å in the O−O RDF. The first maximum in the RDFs is at 1.83 Å (O−H) and 2.78 Å (O−O). In the O−H RDF, a clear second maximum is found at around 3.08 Å. Thus, a hydrogen bond length of 1.83 Å is found. Furthermore, using the intramolecular geometry of the water molecules, we find that this hydrogen bond is almost linear in the carbonyl oxygen−water hydrogen−water oxygen atoms. Similar trends were found for formaldehyde RDFs.[62]

D. Combined (GIAO)-DFT/MM Results. With the proper method and a number of solute−solvent configurations at hand, we now move to the large-scale calculations of the shielding constants of formaldehyde and acetone in aqueous solution. Here, the DFT/MM scheme is used. For the QM part of the systems, we apply the PBE0 functional together with the 6-311++G(2d,2p) basis set. The same force field parameters as in the MD simulation (Table 7) are used for the MM water molecules. The final values of the shielding constants in water are evaluated by a statistical averaging of the corresponding shielding constants over all molecular configurations. The gas-to-aqueous solution shifts of the shielding constants are estimated with respect to the corresponding shielding constants of the solute in vacuum.

1. Formaldehyde. The DFT/MM results for the shielding constants of formaldehyde in aqueous solution averaged over 1200 solute−solvent configurations are presented in Table 8. As a first step, we consider formaldehyde as the QM part of

TABLE 8: PBE0/6-311++G(2d,2p) Isotropic Shielding Constants, σ^O and σ^C, (in ppm) of Formaldehyde Averaged over 1200 Solute−Solvent Configurations[a]

QM part	outer part	no. of configs.	σ^O	δ^O	σ^C	δ^C
for-vac			−432.3		−12.8	
for-sim	PCM-UA0		−385.1	47.2	−26.6	−13.8
for-sim	SPCpol H_2O	1200	−296.3 ± 0.7	136.0 ± 0.7	−36.9 ± 0.1	−24.1 ± 0.1
for-sim + 2 H_2O	SPCpol H_2O	1200	−298.9 ± 0.7	133.4 ± 0.7	−36.2 ± 0.1	−23.4 ± 0.1
for-sim + 4 H_2O	SPCpol H_2O	1200	−301.2 ± 0.7	131.1 ± 0.7	−35.9 ± 0.1	−23.1 ± 0.1

[a] The results are obtained for formaldehyde together with none and the two and four closest water molecules included in the QM part of the DFT/MM scheme. The differences with respect to the corresponding shielding constants in vacuum define the solvation shifts, δ^O and δ^C. The statistical errors are calculated according to $\sigma/\sqrt{N}$ (σ is the standard deviation). Also included are the results for formaldehyde obtained using the PCM model to model solvent effects.

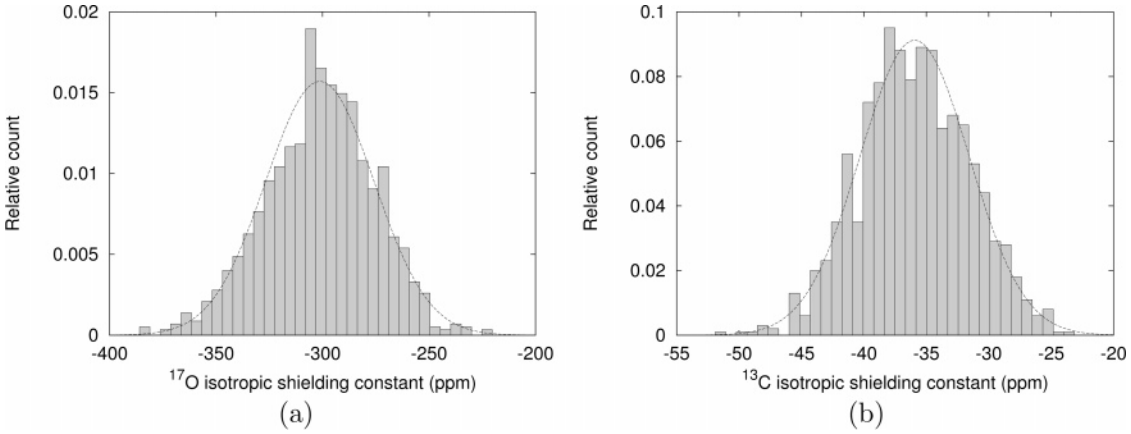

Figure 4. Statistical distribution of the σ^O (a) and σ^C (b) in formaldehyde using 1200 solute−solvent configurations. Formaldehyde and the four closest water molecules were treated quantum mechanically at the PBE0/6-311++G(2d,2p) level.

the system and treat all water molecules classically using the SPCpol molecular potential. The estimated liquid-phase values of −296.3 ± 0.7 ppm for σ^O and −36.9 ± 0.1 ppm for σ^C result in the gas-to-aqueous solution shifts for δ^O and δ^C of 136.0 ± 0.7 and −24.1 ± 0.1 ppm, respectively. As seen in Table 3, the supermolecular approach at the PBE0/aug-cc-pCVTZ level gives shifts of 55.4 ppm for δ^O and −10.4 ppm for δ^C when two water molecules in the energy-minimized structure are treated classically. The electrostatic effect of the more distant solvent molecules is therefore observed to be responsible for a substantial part of the solvation shifts and cannot be neglected.

In the calculations described above, formaldehyde is only perturbed by the electrostatic field generated by the MM water molecules, and intermolecular quantum effects are not taken into account. However, dispersion and short-range repulsion interactions may have a significant impact on the molecular properties of molecules in condensed phases. Quantum effects are thus crucial in order to obtain even qualitative agreement with experiment for the gas-to-liquid shifts of the ^{17}O and ^{1}H shielding constants of liquid water.[28,34,68−70] We have therefore also investigated the effects of nonclassical intermolecular interactions on δ^O and δ^C for formaldehyde. In these calculations, we include two or four explicit water molecules (those closest to the oxygen atom of formaldehyde) into the QM system. The statistically averaged results are collected in Table 8. Including two QM water molecules results in somewhat smaller solvation shifts, decreased by 2.6 ppm for δ^O and −0.7 ppm (negative shift) for δ^C compared to the corresponding results of pure electrostatics. Further extension of the QM system to four water molecules together with formaldehyde leads to a further reduction of δ^O by 2.3 ppm and has a minor effect of −0.3 ppm for δ^C. Therefore, 131.1 ± 0.7 and −23.1 ± 0.1 ppm are our best estimates for the gas-to-aqueous solution shifts of, respectively, $\sigma^O$and σ^C in formaldehyde. In this case, quantum effects are responsible for a reduction in the total solvation shift of σ^O and σ^C by 3.6% and 4.1%, respectively.

In Figure 4, we show the statistical distribution of σ^O and σ^C in formaldehyde over 1200 solute−solvent configurations. In addition, we have plotted the Gaussian probability density function with the mean value and standard deviation taken from the statistical analysis of the computed data. The results refer to the DFT/MM calculation on formaldehyde and four water molecules considered at the DFT level. A spread of ∼170 ppm for σ^O and ∼30 ppm for σ^C is observed. This implies that statistical averaging over an appropriate number of configurations is mandatory in order to obtain reliable values for the shielding constants in liquid phases.

2. Acetone. Having discussed the DFT/MM results for the shielding constants of formaldehyde in aqueous solution, we now turn to the DFT/MM calculations for acetone. In this case, a comparison of the computed numbers with reliable experimental data for the gas-to-aqueous solution shift of σ^O and σ^C in acetone is available, and a well-founded evaluation of the quality of the different models can be made. Moreover, having the molecular configurations from the SPCpol and SPC MD simulations we are in position to test the accuracy of both potentials in the DFT/MM calculations. As in the case of formaldehyde, we first consider a QM acetone surrounded by the MM water molecules described by the SPCpol potential. The DFT/MM values of σ^O and σ^C averaged over 1200 solute−solvent configurations as well as the corresponding solvation shifts, δ^O and δ^C, are presented in Table 9. Experimental solvation shifts are also included in Table 9 for comparison. The MM treatment of all solvent molecules overestimates the result for δ^O in acetone as compared to the experimental data, whereas δ^C is found to be underestimated. The δ^O shift of 79.9 ± 0.7 ppm compares fairly well with the experimental value of 75.5 ppm. The computed δ^C is −15.5 ± 0.1 ppm and

TABLE 9: Statistically Averaged PBE0/6-311++G(2d,2p) Isotropic Shielding Constants, σ^O and σ^C, (in ppm) of Acetone[a]

QM part	outer part	no. of configs.	σ^O	δ^O	σ^C	δ^C
act-vac			−339.2		−21.5	
act-sim	PCM-UA0		−285.6	53.6	−33.2	−11.7
act-sim	SPCpol H_2O	1200	−259.3 ± 0.7	79.9 ± 0.7	−37.0 ± 0.1	−15.5 ± 0.1
act-sim	SPCpol H_2O	700	−259.0 ± 0.9	80.2 ± 0.9	−37.1 ± 0.1	−15.6 ± 0.1
act-sim + 2 H_2O	SPCpol H_2O	700	−258.7 ± 0.8	80.5 ± 0.8	−37.7 ± 0.1	−16.2 ± 0.1
act-sim	TIP3P H_2O	1200	−250.6 ± 0.6	88.6 ± 0.6	−38.2 ± 0.1	−16.7 ± 0.1
act-sim + 2 H_2O	TIP3P H_2O	1200	−251.0 ± 0.6	88.2 ± 0.6	−38.9 ± 0.1	−17.4 ± 0.1
act-sim + 2 H_2O	none	700	−297.3 ± 0.5	41.9 ± 0.5	−31.1 ± 0.1	−9.6 ± 0.1
act-sim + 2 H_2O	PCM-UA0	700	−262.7 ± 0.5	76.5 ± 0.5	−36.6 ± 0.1	−15.1 ± 0.1
act-sim + 2 H_2O	PCM-UFF	700	−250.1 ± 0.5	89.1 ± 0.5	−38.2 ± 0.1	−16.7 ± 0.1
exp				75.5		−18.9

[a] The differences with respect to the corresponding shielding constants in vacuum define the solvation shifts, δ^O and δ^C. The statistical errors are calculated according to $\sigma/\sqrt{N}$ (σ is the standard deviation).

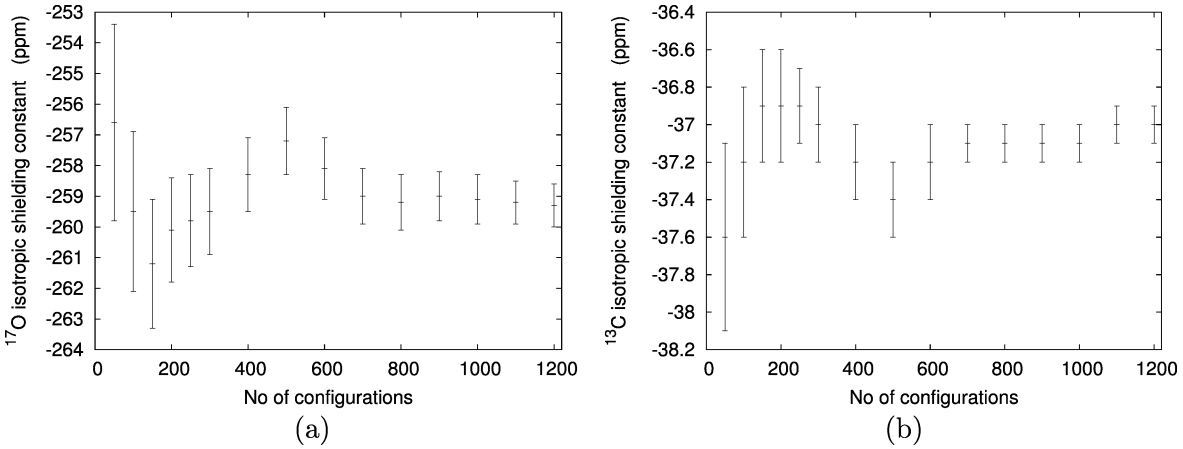

Figure 5. σ^O (a) and σ^C (b) in acetone as a function of the number of molecular configurations included in the statistical averaging. The error bars are calculated according to $\sigma/\sqrt{N}$ (σ stands for the standard deviation).

differs from the experimental solvation shift by −3.4 ppm. To get more accurate results for δ^O and δ^C in acetone, the necessity of including two or three explicit water molecules together with acetone, all treated at the QM level, was stressed in refs 36−38. These findings are in line with our DFT/MM results for δ^O in formaldehyde, where a small down-shifting effect due to the nonclassical intermolecular interactions was observed.

We therefore also performed calculations in which acetone and the two closest water molecules are treated at the QM level. However, we would first like to determine the smallest number of solute−solvent configurations that need to be included in the statistical averaging in order to obtain statistically converged results. In Figure 5, the convergence of the σ^O and σ^C for acetone with respect to the number of solute−solvent configurations included in the statistical averaging is illustrated. Significant changes in the property are observed up to about 600 configurations for σ^O and σ^C. Therefore, including 700 configurations in the averaging procedure would provide statistically converged properties because only small fluctuations are observed beyond this number of configurations. For comparative purposes, we also include the results of calculations averaged over 700 and 1200 molecular configurations in Table 9. The smaller number of configurations used in the statistical averaging leads to somewhat larger statistical errors, whereas the mean values are almost unaffected.

At this point, we want to investigate the convergence of the statistically averaged NMR shielding constants with respect to the number of water molecules included into the molecular configuration. In Figure 6, the shielding constants σ^O and σ^C of acetone for different cutoff distances are displayed. In these calculations, acetone has been considered quantum mechanically, and the results are statistical averages over 700 molecular configurations. As seen from Figure 6, the shielding constants start to converge with a cutoff radius of 10 Å and they are clearly converged for the cutoff distance equal to 12 Å, which is used throughout this work. The cutoff radius of 12 Å includes approximately 230−240 water molecules together with a solute into the molecular configuration.

The extension of the QM part to include acetone and two water molecules has very little effect on both solvation shifts δ^O and δ^C. In fact, the averaged values for δ^O are within the limits of statistical errors when none or two explicit water molecules are included in the QM part of the QM/MM model (see Table 9). In contrast to the observations made for formaldehyde, the magnitudes of the solvation shifts are increasing, though only slightly, when using a QM description of the acetone−water hydrogen bonds. The value of δ^O is shifted slightly from 80.2 ± 0.9 ppm to 80.5 ± 0.8 ppm, and the corresponding δ^C solvation shift is increased by −0.6 ppm with the total value of −16.2 ± 0.1 ppm being −2.7 ppm away from the experimental data. It is possible to refine our results further by applying the QM description for more water molecules together with acetone. However, having in mind the outcome of this for formaldehyde, we expect only minor changes in the results.

A corresponding series of DFT/MM calculations has been carried out by applying the TIP3P MM potential for the classical water molecules. The molecular configurations dumped in the SPC MD simulation were used in these calculations. The isotropic shielding constants obtained by averaging over 1200 configurations and corresponding solvation shifts are presented in Table 9. In line with the SPCpol results, the obtained solvation

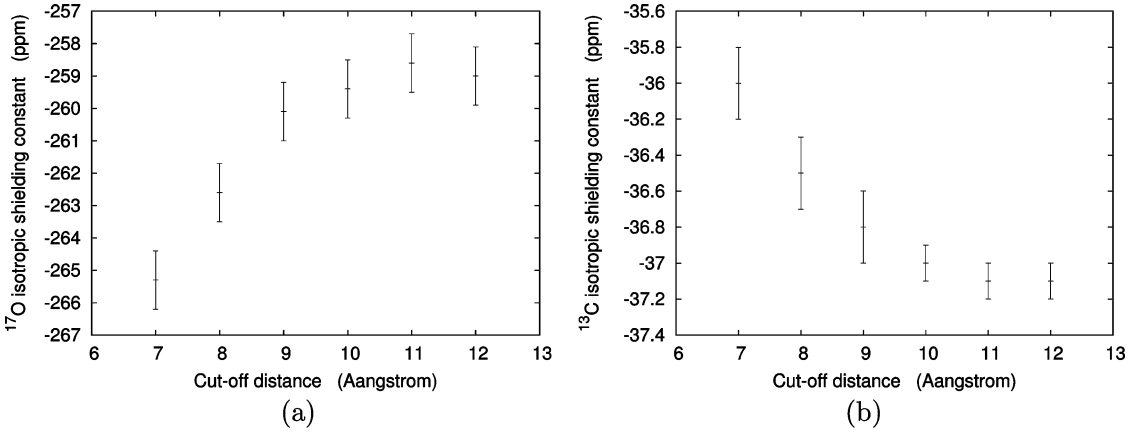

Figure 6. σ^O (a) and σ^C (b) in acetone as a function of the cutoff distance applied to the molecular configurations from the MD simulation. The error bars are calculated according to $\sigma/\sqrt{N}$ (σ stands for the standard deviation).

shifts are almost unchanged when going from zero to two water molecules in the QM part. However, the determined shifts δ^O and δ^C are larger in magnitude compared to the corresponding SPCpol results. The computed δ^O value of 88.2 ± 0.6 ppm (acetone and two water molecules in the QM part) differs from the experimental value by 12.7 ppm. However, our result is in very close agreement with the δ^O value of 87 ppm reported in ref 38. In the latter study, the isotropic shielding constants in aqueous solution are evaluated as a statistical average over a number of small aggregates consisting of acetone and two water molecules extracted from the nonpolarizable MD simulation, and the PCM model was applied to account for the bulk effects. The averaged δ^C value of -17.4 ± 0.1 ppm is -1.2 ppm larger than the corresponding SPCpol result but is still underestimated with respect to the experimental data. We therefore conclude that it is crucial to account for the polarization explicitly in both the MD simulation and the QM/MM calculations in order to obtain reliable isotropic shielding constants of molecules in solutions.

As seen from Table 6, the PBE0/6-311++G(2d,2p) values of δ^O and δ^C for the energy-minimized structure of acetone and two water molecules are underestimated as compared to the experimental data. On the other hand, the inclusion of the PCM in the calculation of the shielding constants leads to a considerable overestimation of the supermolecular result for δ^O, whereas δ^C was reproduced correctly. We would like to consider this approach in more detail by also taking into account the effects of statistics. We first consider 700 molecular configurations consisting of acetone and the two closest water molecules at the PBE0/6-311++G(2d,2p) level, thereby neglecting the effects of the bulk solvent molecules. Afterwords, we refine this model by including the electrostatic solvent effects by the PCM method. The Gaussian 03 program was used for the latter calculations.

The statistically averaged results are collected in Table 9. The statistical effect of two QM water molecules leads to even more underestimated values for δ^O and δ^C as compared to the corresponding numbers for the energy-minimized supermolecular calculations in Table 6. These findings support the assumption that solvent effects have a tendency to be overestimated in the supermolecular approach for geometry-optimized structures. However, the coupling between the PCM-UA0 model for bulk effects with the statistical averaging for dynamical effects gives a very accurate value for δ^O and a somewhat underestimated δ^C (by -3.8 ppm) compared to the experimental data. In contrast, when the more realistic molecular cavities with individual spheres around hydrogen atoms are used (via the PCM-UFF model), the δ^O value is again overestimated by 13.6 ppm as compared to the experimental data. The computed δ^C solvation shift deviates from the corresponding experimental number by -2.2 ppm. A reconsideration of the construction of the PCM cavities for the calculation of NMR shielding constants (and probably other molecular properties) is therefore highly necessary and deserves a separate study.

By observing the DFT/MM results in Tables 8 and 9, one can identify the crucial impact of bulk solvent effects on shielding constants of molecules in liquid phases. In the QM/MM scheme, a number of discrete solvent molecules around the solute are considered, and therefore resulting intermolecular interactions possess directional character. The directional long-range intermolecular interactions are seen to be responsible for a large part of the gas-to-aqueous solution shift of σ^O and σ^C in acetone. In contrast, PCM treats solvent effects in an average way. The straightforward approach to immerse the solute into the DC leads to significantly underestimated results for the solvation shifts δ^O and δ^C for formaldehyde and acetone, as indicated in Tables 8 and 9, respectively. It is therefore necessary to include explicit water molecules together with the solute in the PCM cavity and average over an appropriate number of configurations in order to compensate for the lack of directionality in the intermolecular interactions and obtain satisfactory results for the solvation shifts of the shielding constants. However, a much faster convergence with respect to the number of explicit solvent molecules treated at the QM level within QM/MM compared to the PCM scheme was demonstrated in ref 38, and these observations are corroborated by our results, that is, accurate solvation shifts of shielding constants for acetone are obtained when only treating the solute at the QM level and the solvent at the MM level of theory. It may still be mandatory to include explicit solvent molecules, those closest to the solute, to the QM region of the QM/MM scheme for systems where rather strong hydrogen bonds between the solute and the solvent are formed. This applies for instance in the case of liquid water[28] and partially for formaldehyde in aqueous solution.

IV. Summary

This paper presents calculations of the gas-to-aqueous solution shifts of the ^{17}O and ^{13}C isotropic shielding constants of the carbonyl chromophore in formaldehyde and acetone using a recent (GIAO)-DFT/MM implementation in the electronic structure program Dalton, as well as corresponding results using PCM. The PBE0 exchange-correlation functional was used for

the calculations of the shielding constants. The 6-311++G (2d,2p) basis set was used throughout this study because it was found to reproduce well the shifts in the shielding constants obtained when using extensive correlation-consistent basis sets of quadruple-ζ quality. The DFT/MM calculation of the ^{17}O and ^{13}C isotropic shielding constants in aqueous solution was based on statistical averaging of the corresponding shielding constants over an appropriate number of solute−solvent configurations extracted from the classical MD simulation. We have used the same force field parameters in both the MD simulation and the DFT/MM calculation, and molecular electric polarization was treated either explicitly or implicitly. Within the DFT/MM scheme, we have applied the selected DFT method for either (a) the solute or (b) the solute and two or four explicit water molecules. This investigation utilized 1200 molecular configurations in the statistical averaging for formaldehyde, and 700 configurations were found to give statistically converged results for acetone.

By using the polarizable MM force field for all solvent molecules, we obtained for formaldehyde 136.0 ± 0.7 and -24.1 ± 0.1 ppm for the gas-to-aqueous solution shifts for the isotropic shielding constants of ^{17}O and ^{13}C, respectively. The explicit inclusion of the water molecules closest to the solute (oxygen site) in the QM part of the system was found to lower the magnitude of the solvation shifts for both the ^{17}O and ^{13}C isotropic shielding constants slightly. Our best estimate for the gas-to-aqueous solution shifts of the ^{17}O and ^{13}C isotropic shielding constants in formaldehyde was obtained by considering four explicit water molecules together with formaldehyde at the QM level and is 131.1 ± 0.7 and -23.1 ± 0.1 ppm, respectively. In the case of acetone in aqueous solution, two QM water molecules included in the QM system were found to have only a very small effect on the solvation shifts as compared to the case where all water molecules were treated classically. The computed gas-to-aqueous solution shifts of the ^{17}O and ^{13}C isotropic shielding constants of 80.5 ± 0.8 and -16.2 ± 0.1 ppm, respectively, compare very well with experimental data. Moreover, a broad distribution of the isotropic shielding constants over the molecular configurations was observed, indicating that statistical averaging over an appropriate number of configurations is mandatory. The polarizable MM force field was found to be necessary both in the MD simulation and DFT/MM calculations.

The effects of the bulk solvent molecules were found to be crucial for an accurate reproduction of the solvation shifts of the shielding constants. These can be taken into account using either a dielectric continuum model or a number of discrete classical solvent molecules surrounding the solute. However, a number of explicit solvent molecules together with the solute have to be considered in the PCM model in order to obtain satisfactory results for the solvation shifts of shielding constants. In addition, a recalibration of the PCM cavities appears to be mandatory for the calculation of molecular magnetic properties. In contrast, the DFT/MM scheme provides accurate gas-to-aqueous solution shifts for the shielding constants of acetone when all solvent molecules are considered classically and polarizable MM force fields are used. By comparing the statistically averaged DFT/MM results with the corresponding supermolecular results obtained for the geometry-optimized structures, we have identified the superiority of the former method in the determination of the shielding constants of solutes in aqueous solution. The supermolecular approach based on energy-minimized structures and exploitation of the PCM for modeling the effects of the bulk overestimates the gas-to-aqueous solution shifts of the ^{17}O isotropic shielding constant in acetone significantly. However, the obtained DFT solvation shifts may suffer from the general incapability of DFT methods to treat van der Waals interactions properly, which, according to MP2 test-calculations, lead to a reduction of solvation shifts.

Acknowledgment. We thank the Danish Center for Scientific Computing (DCSC) for the computational resources. K.A. acknowledges support from the EU network NANOQUANT. K.V.M. thanks Forskningsrådet for Natur og Univers (FNU), DCSC and the EU network NANOQUANT for support. O.C. acknowledges support from the Danish national research foundation and DCSC. J.K. and O.C. have been supported by the Lundbeck Foundation and The Danish Natural Science Research Council (Grant No. 21-04-0268). J.K. thanks the Villum Kann Rasmussen foundation for financial support. K.R. has been supported by the Norwegian Research Council through a Strategic University Program in Quantum Chemistry (Grant No. 154011/420) and an YFF Grant (Grant No. 162746/V00).

References and Notes

(1) Pullman, A. In *The New World of Quantum Chemistry*; Pullman, B.; Parr, R., Eds.; Reidel: Dordrecht, The Netherlands, 1976; p 149.
(2) Pullman, A. In *Quantum Theory of Chemical Reactions*; Daudel, R.; Pullman, A.; Salem, L.; Veillard, A., Eds.; Reidel: Dordrecht, The Netherlands, 1981; Vol. 2, p 1.
(3) Kitaura, K.; Morokuma, K. *Int. J. Quantum Chem.* **1976**, *10*, 325.
(4) Warshel, A.; Levitt, M. *J. Mol. Biol.* **1976**, *103*, 227.
(5) Singh, U. C.; Kollman, P. A. *J. Comput. Chem.* **1986**, *7*, 718.
(6) Field, M. J.; Bash, P. A.; Karplus, M. *J. Comput. Chem.* **1990**, *11*, 700.
(7) Thompson, M. A. *J. Phys. Chem.* **1996**, *100*, 14492.
(8) Böttcher, C. *Theory of Electronic Polarization*; Elsevier Scientific: Amsterdam, 1973.
(9) Tomasi, J.; Mennucci, B.; Cammi, R. *Chem. Rev.* **2005**, *105*, 2999.
(10) Allen, M.; Tildesley, D. *Computer Simulation of Liquids*; Clarendon Press: Oxford, 1987.
(11) Car, R.; Parrinello, M. *Phys. Rev. Lett.* **1985**, *55*, 2471.
(12) *Dalton, an ab initio electronic structure program*, release 2.0; 2005. See http://www.kjemi.uio.no/software/dalton/dalton.html.
(13) Kongsted, J.; Osted, A.; Mikkelsen, K. V.; Christiansen, O. *Mol. Phys.* **2002**, *100*, 1813.
(14) Kongsted, J.; Osted, A.; Mikkelsen, K. V.; Christiansen, O. *J. Chem. Phys.* **2002**, *118*, 1620.
(15) Kongsted, J.; Osted, A.; Mikkelsen, K. V.; Christiansen, O. *J. Chem. Phys.* **2003**, *119*, 10519.
(16) Kongsted, J.; Osted, A.; Mikkelsen, K. V.; Christiansen, O. *J. Chem. Phys.* **2004**, *120*, 3787.
(17) Kongsted, J.; Osted, A.; Mikkelsen, K. V.; Åstrand, P.-O.; Christiansen, O. *J. Chem. Phys.* **2004**, *121*, 8435.
(18) Aidas, K.; Kongsted, J.; Osted, A.; Mikkelsen, K. V.; Christiansen, O. *J. Phys. Chem. A* **2005**, *109*, 8001.
(19) Osted, A.; Kongsted, J.; Mikkelsen, K. V.; Åstrand, P.-O.; Christiansen, O. *J. Chem. Phys.* **2006**, *124*, 124503.
(20) Parr, R.; Yang, W. *Density-Functional Theory of Atoms and Molecules;* Oxford University Press Inc.: New York, 1989.
(21) Nielsen, C. B.; Kongsted, J.; Christiansen, O.; Mikkelsen, K. V. *J. Chem. Phys.*, in press, 2007.
(22) Helgaker, T.; Jaszuński, M.; Ruud, K. *Chem. Rev.* **1999**, 99, 293.
(23) Grant, D. M., Harris, R. K., Eds. *Encyclopedia of Nuclear Magnetic Resonance;* Wiley: New York, 1996.
(24) Krishna, N. R., Berliner, L. J., Eds. *Biological Magnetic Resonance;* Kluwer/Plenum: New York, 1998−2003; Vol. 16−17, 20.
(25) Auer, A. A.; Gauss, J.; Stanton, J. F. *J. Chem. Phys.* **2003**, 118, 10407.
(26) Siehl, H.-U.; Müller, T.; Gauss, J. *J. Phys. Org. Chem.* **2003**, *16*, 577.
(27) Wu, A.; Cremer, D.; Gauss, J. *J. Phys. Chem. A* **2003**, *107*, 8737.
(28) Kongsted, J.; Nielsen, C. B.; Mikkelsen, K. V.; Christiansen, O.; Ruud, K. *J. Chem. Phys.* **2007**, *126*, 034510.
(29) London, F. *J. Phys. Radium* **1937**, *8*, 397.
(30) Hameka, H. F. *Rev. Mod. Phys.* **1962**, *34*, 87.
(31) Ditchfield, R. *Mol. Phys.* **1974**, *27*, 789.
(32) Wolinski, K.; Hinton, J. F.; Pulay, P. *J. Am. Chem. Soc.* **1990**, 112, 8251.
(33) Kupka, T.; Kołaski, M.; Pasterna, G.; Ruud, K. *J. Mol. Struct.: THEOCHEM* **1999**, *467*, 63.

(34) Cossi, M.; Crescenzi, O. *J. Chem. Phys.* **2003**, *118*, 8863.
(35) Tiffon, B.; Dubois, J. *Org. Magn. Reson.* **1978**, *11*, 295.
(36) Benzi, C.; Crescenzi, O.; Pavone, M.; Barone, V. *Magn. Reson. Chem.* 2004, *42*, S57.
(37) Crescenzi, O.; Pavone, M.; De Angelis, F.; Barone, V. *J. Phys. Chem. B* **2005**, *109*, 445.
(38) Pavone, M.; Brancato, G.; Morelli, G.; Barone, V. *ChemPhysChem* 2006, *7*, 148.
(39) Buckingham, A. D.; Schaefer, T.; Schneider, W. G. *J. Chem. Phys.* 1960, *32*, 1227.
(40) Salek, P.; Vahtras, O.; Helgaker, T.; Ågren, H. *J. Chem. Phys.* 2002, *117*, 9630.
(41) Doltsinis, N. In *Computational Nanoscience: Do It Yourself!*; Grotendorst, J., Blügel, S., Marx, D., Eds.; NIC Series, John von Neumann Institute for Computing: Jülich, 2006; Vol. 31, pp 357−373.
(42) Linse, P. *Molsim*, an integrated md/mc/bd simulation program belonging to the Molsim package, version 3.3.0; 2001.
(43) Christiansen, O. *MidasCpp*, a molecular interactions and simulation in c++; 2004.
(44) Frisch, M. J.; Trucks, G. W.; Schlegel, H. B.; Scuseria, G. E.; Robb, M. A.; Cheeseman, J. R.; Montgomery, J. A., Jr.; Vreven, T.; Kudin, K. N.; Burant, J. C.; Millam, J. M.; Iyengar, S. S.; Tomasi, J.; Barone, V.; Mennucci, B.; Cossi, M.; Scalmani, G.; Rega, N.; Petersson, G. A.; Nakatsuji, H.; Hada, M.; Ehara, M.; Toyota, K.; Fukuda, R.; Hasegawa, J.; Ishida, M.; Nakajima, T.; Honda, Y.; Kitao, O.; Nakai, H.; Klene, M.; Li, X.; Knox, J. E.; Hratchian, H. P.; Cross, J. B.; Bakken, V.; Adamo, C.; Jaramillo, J.; Gomperts, R.; Stratmann, R. E.; Yazyev, O.; Austin, A. J.; Cammi, R.; Pomelli, C.; Ochterski, J. W.; Ayala, P. Y.; Morokuma, K.; Voth, G. A.; Salvador, P.; Dannenberg, J. J.; Zakrzewski, V. G.; Dapprich, S.; Daniels, A. D.; Strain, M. C.; Farkas, O.; Malick, D. K.; Rabuck, A. D.; Raghavachari, K.; Foresman, J. B.; Ortiz, J. V.; Cui, Q.; Baboul, A. G.; Clifford, S.; Cioslowski, J.; Stefanov, B. B.; Liu, G.; Liashenko, A.; Piskorz, P.; Komaromi, I.; Martin, R. L.; Fox, D. J.; Keith, T.; Al-Laham, M. A.; Peng, C. Y.; Nanayakkara, A.; Challacombe, M.; Gill, P. M. W.; Johnson, B.; Chen, W.; Wong, M. W.; Gonzalez, C.; Pople, J. A. *Gaussian 03*, revision C.02; Gaussian, Inc.: Wallingford, CT, 2004.
(45) Becke, A. D. *J. Chem. Phys.* **1993**, *98*, 5648.
(46) Kendall, R. A.; Dunning, T. H.; Harrison, R. J. *J. Chem. Phys.* **1992**, *96*, 6796.
(47) Schoolery, J. N.; Sharbaugh, A. H. *Phys. Rev.* **1951**, *82*, 95.
(48) Nelson Jr., R. D.; Lide, D. R.; Maryott, A. A. *Selected Values of Electric Dipole Moments for Molecules in the Gas Phase*; NSRDS-NBS10, 1967.
(49) Miertuš, S.; Scrocco, E.; Tomasi, J. *Chem. Phys.* **1981**, 55, 117.
(50) Adamo, C.; Barone, V. *J. Chem. Phys.* **1999**, *110*, 6158.
(51) Handy, N. C.; Cohen, A. J. *Mol. Phys.* **2001**, *157*, 403.
(52) Keal, T. W.; Tozer, D. J. *J. Chem. Phys.* **2003**, *119*, 3015.
(53) Keal, T. W.; Tozer, D. J.; Helgaker, T. *Chem. Phys. Lett.* **2004**, *391*, 374.
(54) Keal, T. W.; Tozer, D. J. *J. Chem. Phys.* **2004**, *121*, 5654.
(55) Dunning, T. H. *J. Chem. Phys.* **1989**, *90*, 1007.
(56) Møller, C.; Plesset, M. S. *Phys. Rev.* **1934**, *46*, 618.
(57) Silvi, B.; Wieczorek, R.; Latajka, Z.; Alikhani, M. E.; Dkhissi, A.; Bouteiller, Y. *J. Chem. Phys.* **1999**, *111*, 6671.
(58) Adamo, C.; Cossi, M.; Barone, V. *J. Mol. Struct.: THEOCHEM* **1999**, *493*, 145.
(59) Frisch, M. J.; Pople, J. A.; Binkley, J. S. *J. Chem. Phys.* **1984**, *80*, 3265.
(60) Cammi, R.; Mennucci, B.; Tomasi, J. *J. Chem. Phys.* **1999**, *110*, 7627.
(61) Mennucci, B.; Martínez, J. M.; Tomasi, J. *J. Phys. Chem. A* **2001**, *105*, 7287.
(62) Kongsted, J.; Osted, A.; Pedersen, T. B.; Mikkelsen, K. V.; Christiansen, O. *J. Phys. Chem. A* **2004**, *108*, 8624.
(63) Billing, G. D.; Mikkelsen, K. V. *Chem. Phys.* **1994**, *182*, 249.
(64) Breneman, C. M.; Wiberg, K. B. *J. Comput. Chem.* **1990**, *11*, 361.
(65) Ahlström, P.; Wallqvist, A.; Engström, S.; Jönsson, B. *Mol. Phys.* **1989**, *68*, 563.
(66) Jorgensen, W. L. *J. Am. Chem. Soc.* **1981**, *103*, 335.
(67) Jorgensen, W. L.; Briggs, J. M.; Contreras, M. L. *J. Phys. Chem.* 1990, *94*, 1683.
(68) Sebastiani, D.; Rothlisberger, U. *J. Phys. Chem. B* **2004**, *108*, 2807.
(69) Yamazaki, T.; Sato, H.; Hirata, F. *J. Chem. Phys.* **2001**, *115*, 8949.
(70) Mikkelsen, K. V.; Ruud, K.; Helgaker, T. *Chem. Phys. Lett.* **1996**, *253*, 443.
(71) Yamada, K.; Nakagawa, T.; Kuchitsu, K.; Morino, Y. *J. Mol. Spectrosc.* **1971**, *38*, 70.
(72) Hilderbrandt, R. L.; Andreassen, A. L.; Bauer, S. H. *J. Phys. Chem.* **1970**, *74*, 1586.